Desalination and Water Treatment
www.deswater.com

doi: 10.5004/dwt.2019.23490

140 (2019) 312–325
February

Adsorption ability of chelating resin Purolite S930 for removal of metal complex azo dye from aqueous solutions

Danutė Kaušpėdienė[a,*], Audronė Gefenienė[a,b], Romas Ragauskas[a]

[a]*Institute of Chemistry of Center for Physical Sciences and Technology, Vilnius, Lithuania, emails: danute.kauspediene@ftmc.lt (D. Kaušpėdienė), romas.ragauskas@ftmc.lt (R. Ragauskas)*
[b]*Lithuanian University of Educational Sciences, Vilnius, Lithuania, emails: audrone.gefeniene@ftmc.lt, audrone.gefeniene@leu.lt (A. Gefenienė)*

Received 25 May 2018; Accepted 18 November 2018

ABSTRACT

The abilities of the macroporous chelating resin containing iminodiacetic groups (Purolite S930) and the weak basic anion exchanger Purolite A847 to remove the chromium complex dye (LnCr) from aqueous solutions in the batch system have been compared depending on the dye concentration, pH, reaction time and temperature. The maximum capacities (q_{eq}) for Purolite S 930 at pH = 2 and pH = 7 (1.5 and 2.0 mg/g, respectively) were lower as compared with the q_{eq} for Purolite A847 (2.1 and 2.25 mg/g, respectively). The thermodynamic parameters (negative values of $\Delta S°$, $\Delta G°$) and values of activation energy (E_a) have revealed that LnCr dye removal using both resins is an exothermic, spontaneous ion exchange in conjunction with physical adsorption ($\Delta H°$ from –4.3 to –17.29 kJ mol^{-1}). The FTIR spectra of unloaded and LnCr dye loaded anion exchanger Purolite A847 confirms the ion exchange and physical adsorption mechanisms. Isotherms and kinetic modeling studies demonstrate that the experimental data obtained for dye LnCr sorption on both resins well fit the Langmuir and Freundlich isotherms and pseudo second-order rate and intraparticle diffusion models. The rate of dye adsorption on both adsorbents is controlled by the co-acting of external mass transfer at the beginning of the process and then by intraparticle diffusion.

Keywords: Chromium complex dye; Sorption; Chelating resin; Weakly basic anion exchanger

1. Introduction

The metal complex dyes used for dyeing of carpets, wool, polyamide, nylon, polyester fiber as well as for anodizing industry often pose environment problems arising from inadequately treated wastewater discharged into environmental water bodies [1,2]. This is related to the discharged colored water and to the hazardous carcinogenic properties of heavy metals and amines formed by reductive cleavage of azo groups of dyes [3–5]. Therefore, to avoid them from release into the environment and for water reuse in the industrial process, a complete removal of these hazardous dyes from wastewaters is necessary [6,7].

Many chemical and physical methods (coagulation, precipitation, filtration, membrane separation, electrodialysis, photochemical degradation, biological treatment, oxidation, and adsorption) have been used for the removal of dyes from wastewaters. Nevertheless these methods, except adsorption, are of limited application because of expensiveness of the technologies. Adsorption using various adsorbents is one of several ways that facilitates the removal of harmful carcinogenic metal ions and azo compounds. Moreover, adsorption is one of the most effective methods that are applicable in the industry for the return of used water to the production process. Its superiority over other techniques can be assessed in terms of initial costs, flexibility, and simplicity of design, ease

* Corresponding author.

of operation, intensity to toxic pollutants, and the advantage of not leading to harmful products [8,9]. Adsorption of dye using commercial ion exchange resins is a practical method for the removal of dyes from wastewaters and recycling water when compared with the widely used adsorption onto commercial activated carbon. Its main advantages are as follows: the ion exchangers are not spent during the regeneration, recovery of the process water, and removal of a soluble dye.

The removal of acid and reactive dye anions using different anion exchangers (strong and weak basic with gel or macroporous structures of styrene-divinylbenzene or acrylic matrices) was described in [10–19]. The authors have proven that in the dye removal the ion-exchange mechanisms are not predominant; some other mechanisms such as the repulsion between the dye molecules and/or repulsion between the anion exchange matrix, and the dye molecules play a significant role. Particular attention was focused on the competition between the acid dye (Methyl Orange, Orange II, Orange G) and metal anions (CrO_4^{2-}) using the strong basic anion exchanger Amberlite® IRN-78 [19]. It was found, that the decrease in metal anion adsorption increased dye removal, which resulted from the competition.

Recently, novel nanocomposite-based sorbents have been prepared and used for the removal of dyes. The polyaniline/γ-alumina nanocomposite was synthesized by 'in situ' polymerization of aniline in the presence of γ-Al_2O_3 nanoparticles. Batch adsorption experiments were conducted to study the removal of three different anionic dyes: Reactive Red 194 (azo), Acid Blue 62 (anthraquinone) and Direct Blue 199 (phthalocyanine class) from aqueous solutions. The maximum capacities (Q_e, mg/g) obtained for the synthesized nanocomposite (dosage 0.06 g/50 mL) for Reactive Red 194 (azo), Acid Blue 62 (anthraquinone) and Direct Blue 199 (phthalocyanine class) from aqueous solutions (C_0 = 50–1,100 mg/L) were high: 72; 1,000 and 222 mg/g, respectively [20].

The combined adsorption and photocatalytic activity of the prepared polyaniline Zr(IV) selenotungstophosphate nanocomposite was investigated for degradation and removal of methylene blue and malachite green [21].

Magnetic properties of adsorbents enable easy separation of the solid phase from the adsorption medium by an external magnet. Therefore, various composite materials were prepared for the removal of pollutants. Malachite green dye removal by trisodium citrate based magnetite nanocomposite (Fe_3O_4–TSC) was studied by the batch method. After the treatment of malachite green dye solution, the sorbent can be separated using an external magnetic field [22].

Magnetic/silica composite particles were modified with (3-aminopropyl) triethoxysilane, grafted with poly(glycidyl methacrylate) and functionalized with tris(2-aminoethyl) amine. The adsorption of two direct dyes, Direct Blue 6 and Direct Black 38, was investigated under various experimental conditions. Electrostatic interactions and hydrogen bonding between the functional groups of the magnetic particles and sulfonate groups of the dyes were reported [23].

Novel sorbents from the low cost and environmentally friendly materials were also extensively studied for their ability to remove color from wastewater. A tropical brown macroalga *Nizamuddinia zanardinii* was used in Methylene blue dye sorption and desorption studies. The results of this study have indicated that brown macroalga could be an efficient sorbent for the removal of basic dyes from aqueous solutions [24]. Native and chemically modified fungal biomasses of *Funalia trogii* were tested for the removal of Congo Red dye from aqueous solutions. The results showed that biomass especially that modified with triethylenetetraamine demonstrated an excellent dye removal performance [25].

The removal of tartrazine anionic azo dye using masau (*Ziziphus mauritiana*) stone biomass as a novel biosorbent was investigated and optimized. The biosorption proceeds mainly due to the electrostatic attractions of the tartrazine molecules with protonated functional groups such as hydroxyl, carbonyl and amine groups of the masau stone [26].

The lignin–chitosan materials were applied to develop a novel adsorbent, activated lignin–chitosan extruded pellets, for cationic dye methylene blue adsorption. Electrostatic attractions and chemical interactions were observed between amino and hydroxyl groups of the produced adsorbent and amine groups of the dye [27].

The biomaterial *Phoenix dactylifera* seeds were carbonized and an eco-friendly adsorbent was prepared via microwave-assisted chemical activation. The viability of the obtained activated carbon for the remediation of Congo red (CR) acid dye from aqueous solutions was examined [28].

The adsorption of Disperse Red 60 dye by the free Lentinus concinnus biomass and that immobilized to carboxymethyl cellulose was studied. It was determined that the composite beads have a high potential for the dye removal [29].

Magnetic (poly(glycidyl methacrylate-ethylene glycol dimethacrylate) resin was prepared and modified using the tris(2-aminoethyl)amine ligand. The synthesized resin was applied to the adsorption of Reactive Green 5 and Reactive Brown 10 metal complexed azo dyes. Experimental results suggest that a high adsorption capacity for metal complexed dyes in acidic solution can be attributed to the electrostatic interaction and hydrogen bonding between the positively charged amino groups of the resin and the negatively charged sulfonate groups of metal complexed dyes [30].

Taking into account that the chelating resins depending on solution pH exhibit anionic, cationic or amphoteric properties [31–39], in this study an attempt has been made to chelating resin containing iminodiacetic acid functional groups and a nitrogen atom as a possible adsorbent for the metal complex dye. It is known that at pH ~ 2.0 the nitrogen atom and the two carboxylic groups present in the iminodiacetic chelating resin are protonated; therefore, the latter behaves as a weakly basic anion exchanger (pH = 2.21: $RCH_2HN^+(CH_2COOH)_2$). Therefore, iminodiacetic chelating resins in an acidic medium should adsorb the dye anions similar to weak basic anion exchangers [8,11,29]. While, at pH ~ 12, the nitrogen atom and the two carboxylic groups are deprotonated – the ion exchanger behaves as a typical weakly acidic cation exchanger (pH = 12.3: $RCH_2HN(CH_2COO^-)_2$). For pH medium values, the iminodiacetic resin behaves as an amphoteric ion exchanger (pH = 7.41: $RCH_2HN^+(CH_2COO^-)_2$). The iminodiacetic groups provide electron pairs, which react with divalent metals to form a stable coordination covalent bond. While adsorption of trivalent metal ions on iminodiacetic resins proceeds according to the following selectivity order: $Sc^{3+} > Ga^{3+} > In^{3+} > Fe^{3+} > Y^{3+} > La^{3+} > Al^{3+}$ [40].

There is scarce information in the literature concerning the usage of commercial chelating resins for the simultaneous removal of dye and heavy metal ions. Special attention is

paid to the development of new sorbents. For this purpose, the cross-linked nano-chelating resin was synthesized and proofed as a suitable adsorbent for simultaneous removal of dye and heavy metal ions [9]. The detected affinity order of metal ions was as follows: $Cu^{2+} > Cd^{2+} > Hg^{2+}$. The adsorption capacities toward three commercial azo dyes such as acid yellow 42, acid red 151 and mordant blue 9 containing functional groups such as –N=N–, chlorine oxadiazine and sulfate on that resin were also investigated. The maximum adsorption from all the dyes investigated was obtained for the dye acid yellow 42 equal to 91%. A new chelating resin was prepared from Amberlite XAD-4 modified with malachite green and proofed as adsorbent for the removal of cyanide and zinc from electroplating wastewater. The cyanide was successfully removed from the wastewater in the packed bed with the chelating resin to the cyanide effluent concentration of 0.2 mg L^{-1} at 110 bed volume from the mixture containing 200 mg L^{-1} cyanide and 100 mg L^{-1} zinc [41].

Polymeric resins, including chelating iminodiacetic resins, can be used to develop enhanced dye removal combining the physical–chemical and adsorption methods [42,43]. The chemical oxidation combined with ion exchange has a significant potential as a process to recycle or recover metal from textile wastewaters [44]. The possibility to use chelating iminodiacetic resins in the oxidative-adsorption method for the removal of metal complex dye was proofed. Decolorization and degradation of the copper phthalocyanine dye was achieved by the oxidative procedure using a potassium permanganate solution. The dye removal was completed by adsorption of copper (II) ions onto the chelating resin Purolite S 930.

Commercial Purolite S 930 is used to remove heavy metals and other cations from wastewater since it is a chelating resin and contains functional iminodiacetic groups protonated in the acidic medium, thus there is no need to perform any modification of this widely used sorbent. The functional groups bearing a positive charge can be introduced in the entrapment process of the metal complex dye anions. To our knowledge, the sorption of dyes, including metal complex dyes, by the commercial chelating ion exchange resin Purolite S 930 has not been investigated yet.

In this paper, therefore, we aimed at investigating the potential of the chelating iminodiacetic resin Purolite S930 in the removal of the chromium complex dye LnCr (Lanasyn Navy M-DNL) from aqueous solutions. The effects of the initial dye concentrations, contact time and solution pH as well as influence of temperature on dye adsorption on Purolite S930 were proved and compared with those on Purolite A847 in batch experiments.

2. Materials and methods

2.1. Materials

The tested chromium complex dye (LnCr) was the commercial textile dye anionic Lanasyn Navy M-DNL (1:2 chromium monoazo complex (trisodium bis[3-hydroxy-[(2-hydroxy-1-naphthyl)azo]naphthalene-1-sulphonato(3-)]chromate(3-); molecular mass 834 g/mol; λ_{max} 616 nm), which was purchased from Clariant Produkte AG (Switzerland). The concentration of chromium complex in the dye is approximately 60% that was used to convert all data into the true values. An accurately weighted quantity of the dye was dissolved in deionized water to prepare the stock solution. Experimental solutions of the desired concentrations were obtained by successive dilutions. In order to obtain the dye solutions at different initial pH, small amounts of 1 M HCl or 1 M NaOH were added. The structure of the dye is displayed in Fig. 1

On the other hand, LnCr contained uncomplexed and potentially bioavailable Cr(III), but did not have any toxic Cr(VI) present in the samples [46].

Sorption experiments were observed using the chelating Purolite S 930 resin and weak basic anion exchanger Purolite A847 purchased from Purolite International Ltd. The characteristics of the resins are presented in Table 1.

Prior to use, the resins were rinsed with deionized water to eliminate all impurities and convert the Purolite S 930 resin to the H-form using 7% HCl, whereas to convert Purolite A847 to the OH-form 5% NaOH was used for 1 h. This was followed by rinsing with deionized water. Both the H-form of Purolite S930 and OH-form of Purolite A847 were dried at 50°C for 3 h and stored at room temperature.

2.2. Sorption studies in batch experiment

Experiments were carried out in the batch by mixing 0.5 g of the OH-form of Purolite A847 or 0.5 g of the H-form of Purolite S930 with 25 mL of an aqueous dye solution of a given initial concentration for 5–360 min. At the end of the predetermined time interval, the sorbents were removed by centrifugation and the residual concentration of dye ascertained by a UV-Vis Spectrometer Cintra 101 (GBS Scientific Equipment (USA) LLS) at the respective λ_{max} value, which is 616 nm for this dye. The dye concentration was calculated from a calibration curve.

All the measurements were repeated three times to ensure the reproducibility of the results. The mean of these three data along with the standard deviation were used to calculate the color removal R_e (%), sorption capacity of sorbent q_t (mmol/g) at the phase contact time t, q_{eq} (mmol/g) at phase contact time for attainment of equilibrium, the distribution coefficient K_d (mL/g):

$$R_e = \frac{C_{eq}}{C_0} \times 100 \quad (1)$$

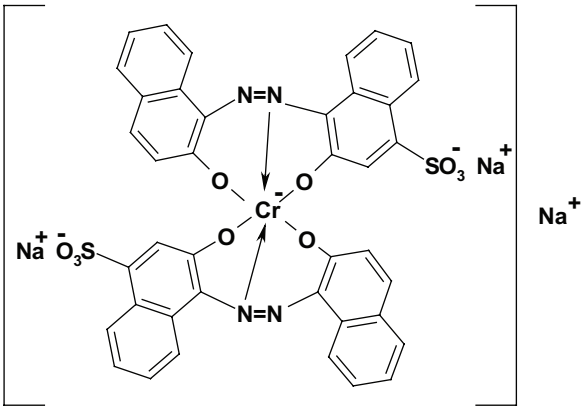

Fig. 1. Structure of the Lanasyn Navy M-DNL dye [45].

$$q_{t(\mathrm{eq})} = \frac{\left(C_0 - C_{t(\mathrm{eq})}\right)V}{m} \quad (2)$$

$$K_d = \frac{q_{\mathrm{eq}}}{C_{\mathrm{eq}}} \quad (3)$$

where C_0 and C_t are the concentrations (mmol/L) of the dye in the solution before and after sorption, respectively, C_{eq} is the dye concentration at equilibrium (mmol/L), V is the volume of the solution (mL) and m is the mass of the dry anion exchanger (g), K_d is the distribution coefficient.

Kinetic values of adsorption were determined by analyzing sorption capacity of the dye under constant shaking (at a speed of 400 rpm) 100 μmol/L dye solutions with 0.5 g mass of sorbent at different time intervals and temperatures 293–333 K.

The concentration of chromium was determined using an ICP optical emission spectrometer (Optima 7000DV, PerkinElmer, USA).

The chemical oxygen demand (COD) values that meet the concentration of all the organic substances present in dye solutions were determined using a Spectroquant TR 320 – Spectroquant Picco analyser.

The surface morphology of the adsorbents was studied by using a scanning electron microscope EVO 50EP (Carl Zeiss SMT AG, Germany) equipped with energy and wave dispersive X-ray spectrometers (Oxford Instruments, UK) and a secondary electron detector (low vacuum mode, 10 kV, 50 Pa, working distance 10 mm).

The infrared spectra of the unloaded and dye-loaded adsorbents were recorded by means of a FTIR spectrometer (PerkinElmer, USA) with a diamond cell: detector-MTC (Mercury–Cadmium–Telluride), source – MIR (Mid Infra-Red), resolution 4 cm^{-1}, the number of scans –50, turning the IR flux, wave range of 4,000–650 cm^{-1}.

3. Results and discussion

3.1. Effect of the initial solution concentration and pH

Comparison of the equilibrium pH values obtained for the sorption of LnCr on the chelating resin Purolite S 930 and weakly basic anion exchanger Purolite A847 shows how it depends on the solution concentration and nature of the functional group present on the resin (Fig. 2).

In the case of anion exchanger Purolite A847 contact with dye solution, the pH rate increased from pH = 2 to pH = 3.2 and from pH = 7 to pH = 9.2 due to the formation of OH^-, which indicates ion exchange. Meanwhile, Purolite S930 virtually had no effect on solution pH (pH = 2 before and pH = 2.1 after). Whereas the decrease in pH value from pH = 7.6 to pH = 7 was possibly due to the deprotonation of the iminodiacetic groups. There is evidence that at medium pH values, the iminodiacetic resin behaves as an amphoteric ion exchanger (pH = 7.41:$RCH_2HN^+(CH_2COO^-)_2$).

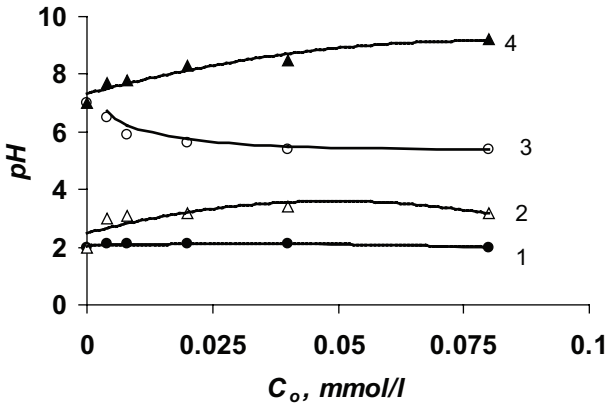

Fig. 2. pH at the equilibrium dependence by sorption on Purolite S930 and Purolite A847 from the initial concentration of LnCr in the solution. Initial dye solution pH = 2 (curves 1, 2) and pH = 7.6 (curves 3, 4).

Table 1
Typical physical and chemical characteristics of the chelating resin Purolite S 930 [47,48]

	Purolite S930	Purolite A847
Polymer structure	Macroporous polystyrene – divinylbenzene	Gel, polyacrylic – divinylbenzene
Appearance	Opaque beige spheres	Opaque beige spheres
Functional group	Iminodiacetic	Tertiary amine
Ionic form	Na^+	OH^-
Total capacity (meq/mL)	1.1	1.6
BET surface area (m^2/g)	20.61	4.05
Average pore diameter (nm)	5.49	7.1
Reversible swelling, H Na (max)	<20%	<20%
Specific gravity, g/mL	1.17	1.06
Shipping weight (approximately), g/L	710–745	680–700
Temperature limit, °C	70	40
pH range	H^+ form 2–6; Na^+ form 6–11	0–9
Principal applications	Heavy metal removal from ores, galvanic plating solutions, picking bath and effluents, various organic or inorganic chemical products.	Demineralization of water high in organic matter

In the case of slightly acidic aqueous solutions, LnCr was dissolved and the strongly sulfonated group of the chromium complex dye ($R'(SO_3)_2Na_2$) was dissociated and converted to anionic dye ions [49]:

$$R'(SO_3)_2Na_2 + 2HCl \rightarrow R'(SO_3)_2^{2-} + 2NaCl + 2H^+ \quad (4)$$

The LnCr dye sorption mechanism onto both sorbents in an acidic medium may be attributed to the chemical reaction (ion exchange) between the protonated amino groups $–N^+H(CH_3)_2$ in the OH-form anion exchanger Purolite A847, $-N^+H(CH_3COOH)_2$ in the H-form of Purolite S 930 and the dye anions ($R'(SO_3)_2^{2-}$):

$$–2\,N^+H(CH_3)_2^- + R'(SO_3)_2^{2-} \rightarrow –2NH(CH_3)_2\,(SO_3)_2R' \quad (5)$$

The chemical reaction between the protonated amino groups and the LnCr dye anions confirms the FTIR spectra of the unloaded and LnCr dye-loaded anion exchanger Purolite A847 at pH = 2. The measured FTIR spectra (figure not presented) were analyzed and compared with the spectra of similar dyes and sorbents [10,50]. Wave numbers for the dominant peak from FTIR spectra are presented in Table 2.

The characteristic peaks for LnCr dye (Table 2) are as follows: an average intensity at 1,458 cm^{-1} (corresponding to matrix C–N groups), medium intensity at 1,419 cm^{-1} (corresponding to matrix C=C groups), medium 1,578 and 1,553 cm^{-1} (corresponding to matrix N=N groups), medium intensities at 1,289 and 1,340 cm^{-1} (corresponding to matrix N–N groups), with a mean intensity at 1,140 cm^{-1} (corresponding to matrix C–O– groups) and a medium intensity at 1,048 cm^{-1} (corresponding to SO_3^- groups).

The characteristic peaks for unloaded Purolite A847 around 3,393 and 2,710 cm^{-1} for –NH stretching vibrations representing the functional group ($–NH^+(CH_3)_2$) (Table 2). The bands representing the anion exchanger matrix are at about 1,647 and 1,715 cm^{-1} – (related to the vibration of –C=O groups), at about 3,073 and 2,956 cm^{-1} (related to the stretching vibrations of the ring C–H bonds) and at about 1,479 cm^{-1} and 1,091 bands, related to the vibration of C–N groups, were recorded.

Table 2
Wave number (cm^{-1}) for the dominant peak from FTIR for LnCr dye sorption onto Purolite A847 at pH = 2

Functional group	LnCr dye	Purolite A847 unloaded	Purolite A847 dye-loaded
C–N	1,458		
C=C	1,419		
N=N	1,578; 1,553		
N–N	1,290; 1,340		
C–O	1,140		
SO_3	1,048	–	1,042
C–H		3,079	3,083
$C–H_2$		2,936	2,963
C=O		1,650	1,650
C–N		1,479	1,469
N–H		2,710	2,720

Whereas in the FTIR spectrum of the dye-loaded anion exchanger a shift from the peaks at 2,710 and 1,479 cm^{-1} is seen (Table 2). Additionally, in the spectrum of the dye-loaded anion exchanger, the vibration at 1,042 cm^{-1} related to the $–SO_3^-$ groups in LnCr was detected. This could be due to new bonds formed between the anion of dye ($R'(SO_3)_3^{2-}$) and the protonated amino groups ($–NH^+(CH_3)_2$). Therefore, the LnCr dye sorption both onto Purolite A847 and Purolite S930 in an acidic media may be considered as conventional ion exchange between the protonated amino groups and the dye anions.

However, the structure of dye molecule and its size is also important when the exchange of large organic anions such as dye molecules is concerned. Therefore to explain the behavior of LnCr dye in the removal process not only the conventional exchange mechanism should be applied but also a physical mechanism involving van der Waals interaction and hydrogen bonding, due to the structure of dye and sorbent (such as the presence of aromatic rings and chemical groups). The hydrophobic surface of the anion exchanger with the styrene–divinylbenzene matrix provides van der Waals interaction sites, while the amine groups provide proton acceptors for hydrogen bonding, both of which could affect the sorption capacity and attractive forces [51]. Van der Waals interactions are here understood as the type of hydrophobic interactions so attachment through the π–π interactions between the aromatic ring of the dye molecule and the phenyl ring on the divinylbenzene matrix of the anion exchanger is considered [52]. The presence of double bonds promotes the interaction between the dye and anion exchanger macromolecule. The double bonds in LnCr dye molecules were detected (Table 2) at bands around 1,419 and 1,420 cm^{-1} for the C=C groups and at 1,578 and 1,553 cm^{-1} for the N=N groups.

As shown in Fig. 3, the pH and the concentration of the initial LnCr solution affect the distribution coefficient (K_d) and the color removal efficiency (R_e, %) on Purolite S930.

The LnCr color removal (R_e, %) using Purolite S930, calculated according to Eq. (1), increases, but the distribution coefficient K_d (Eq. (3)) decreases with increasing initial concentration. The LnCr color removal using Purolite S930 at pH = 2 is about 1.8–2.5 times greater than that at pH = 7. The K_d values decrease with an increase in initial dye concentration. In the area of higher concentrations, the decrease in dye concentration in the solid phase is caused by insufficiency of free sorption sites [53].

The effect of dye equilibrium solution concentrations on the sorption capacity of Purolite S930 is shown in Fig. 4. Purolite S 930 effectively removes LnCr at low initial concentrations; at higher concentrations the isotherms reach a maximum capacity as indicated by the plateau of the data. The maximum capacities (q_{eq}) for Purolite S 930 obtained at solution pH = 2 are slightly lower than q_{eq} for Purolite A847 – 2.1 and 2.25 mg/g, respectively. The same tendency was observed at solution pH = 7–1.5 mg/g for Purolite S 930 and 2.0 mg/g for Purolite A847. We did not find any literature data on the peculiarities of the sorption of metal complex dye by chelating ion exchangers, therefore we can only compare our results with those obtained using weakly basic anion exchangers for various non-complexed dyes. Furthermore, sorption capacity values depend not only on the type of ion exchanger and dye, but also on the experimental conditions, i.e., concentration of sorbent and sorbate in the solution.

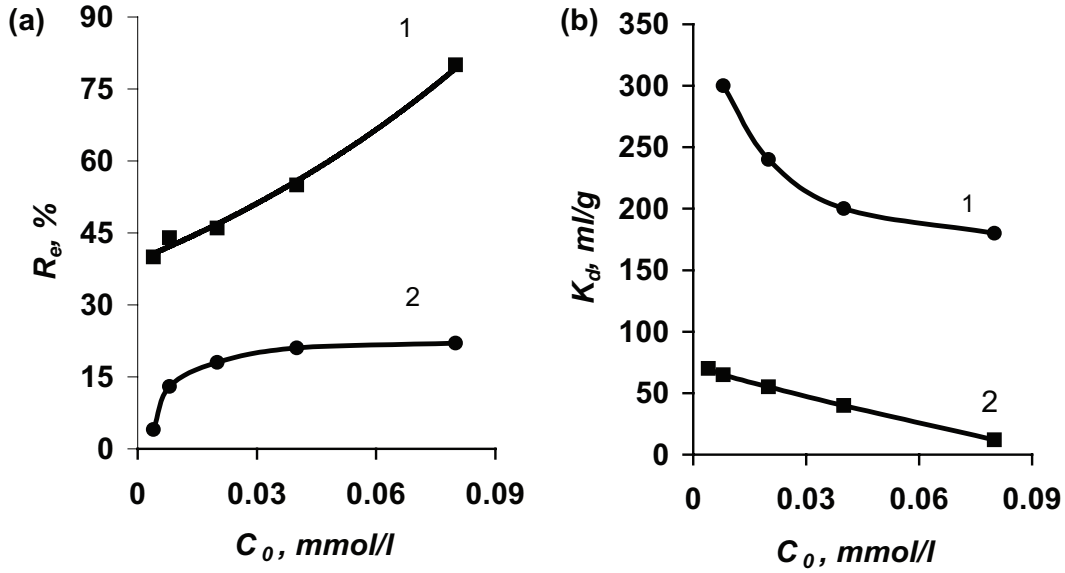

Fig. 3. Dependence of the color removal efficiency (R_e) (a) and distribution coefficient (K_d) (b) on the initial concentration of LnCr in the solution during the sorption on Purolite S 930. Initial dye solution pH = 2 (curves 1) and pH = 7 (curves 2).

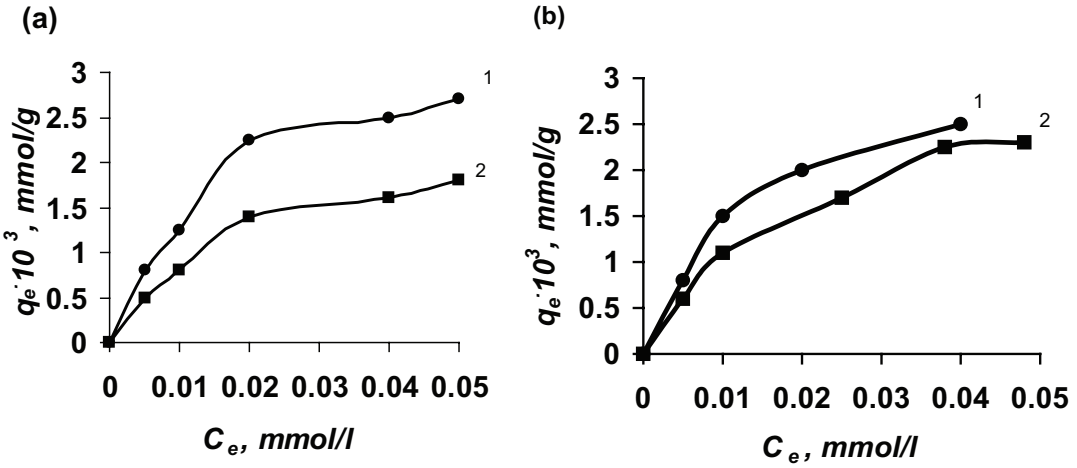

Fig. 4. Isotherms of LnCr dye sorption on Purolite S 930 (a) and Purolite A847 (b) obtained at pH = 2 (1) and pH = 7 (2). Experimental conditions: duration of interaction – 1 d, T – 20°C at pH = 2 (1) and pH = 7 (2).

The sorption capacity of weakly basic Amberlite FPA51 for Sunset Yellow food dye was determined [16]. Sorption experiments were conducted at a solid/liquid ratio of 0.01, by adding 0.25 g of the resin to 25 mL of dye solution. The amount of dye sorbed at equilibrium from the solution with the initial concentration of 100 mg/L was 9.9 mg/g. The weakly basic Amberlyst A-21 anion exchanger was tested for the removal of SPADNS azo dye [14]. It was found that under similar experimental conditions the maximum sorption capacity of 8 mg/g could be reached. The sorption capacity of the same weakly basic anion exchanger Amberlyst A-21 toward Acid Orange 7 and Acid Orange 10 was 5 mg/g at the initial dye concentration of 50 mg/L [54].

The comparison of the concentrations of hazardous components such as chromium and all organic substances COD in the treated dye solutions at pH = 2 using Purolite S930 and Purolite A847 is shown in Table 3.

Table 3
Comparison of the purified LnCr dye solution parameters using Purolite S930 or Purolite A847. Initial solution pH 2, contact time 1 h and temperature 20°C. Conditions: initial LnCr dye concentration 0.08 mmol/L (Cr = 15.40 mg/L; COD = 735 mgO_2/L; T – 20°C; pH_0 = 2; 0.5 g sorbent; LnCr dye solution volume – 25 mL

Parameter	Purolite A847	Purolite S 930
Cr concentration, mg/L	0	1.04
COD, mgO_2/L	0	140
pH	3.2	2.0

It is evident that at the initial pH 2 maximum removals of hazardous components such as chromium (residual concentration lower than 0.1 mg/L) and organic compounds (values of chemical oxygen demand lower than 100 mgO_2/L)

observed for Purolite A847 complies with the requirements for waste water effluents.

However, chelating iminodiacetic Purolite S930 eliminates these hazardous components insufficiently as some chromium and organic compounds remain in the purified solution due to the non-adsorbed dye.

Preliminary the bath regeneration tests of Purolite A847 were conducted using such regenerants as methanol, ethanol, 4% NaOH, or 4% NaOH with methanol or ethanol (1:1), while the tests of LnCr dye recovery from Purolite S 930 were carried out using 7% HCl, 7% HCl with methanol or ethanol (1:1). It has been found that the most effective regenerant for the LnCr dye from Purolite A847 is 4% NaOH with methanol (1:1), while 7% HCl with methanol (1:1) is the most suitable regenerant from Purolite S930.

3.2. Effect of contact time and temperature

Kinetic studies were conducted to reveal the relation between the physical–chemical characteristics of the sorbents and their performance in the removal of LnCr dye. The time-dependent behavior of the dye adsorption was examined by varying contact time between the adsorbent and dye solution in the range of 5–60 min and is presented in Fig. 5.

The amount of sorbed LnCr dye (q_t, mmol/g) plotted as a function of contact time t (Fig. 5) showed that at the initial pH = 2 and a constant temperature the equilibrium between the LnCr and Purolite AS930 was attained later (within shaking 30 min) than between the LnCr and Purolite A847 (within 20 min). From the results obtained, it is clear that the course of sorption is rapid at the initial stage and becomes slow in later stages until equilibrium is attained. This is evident from

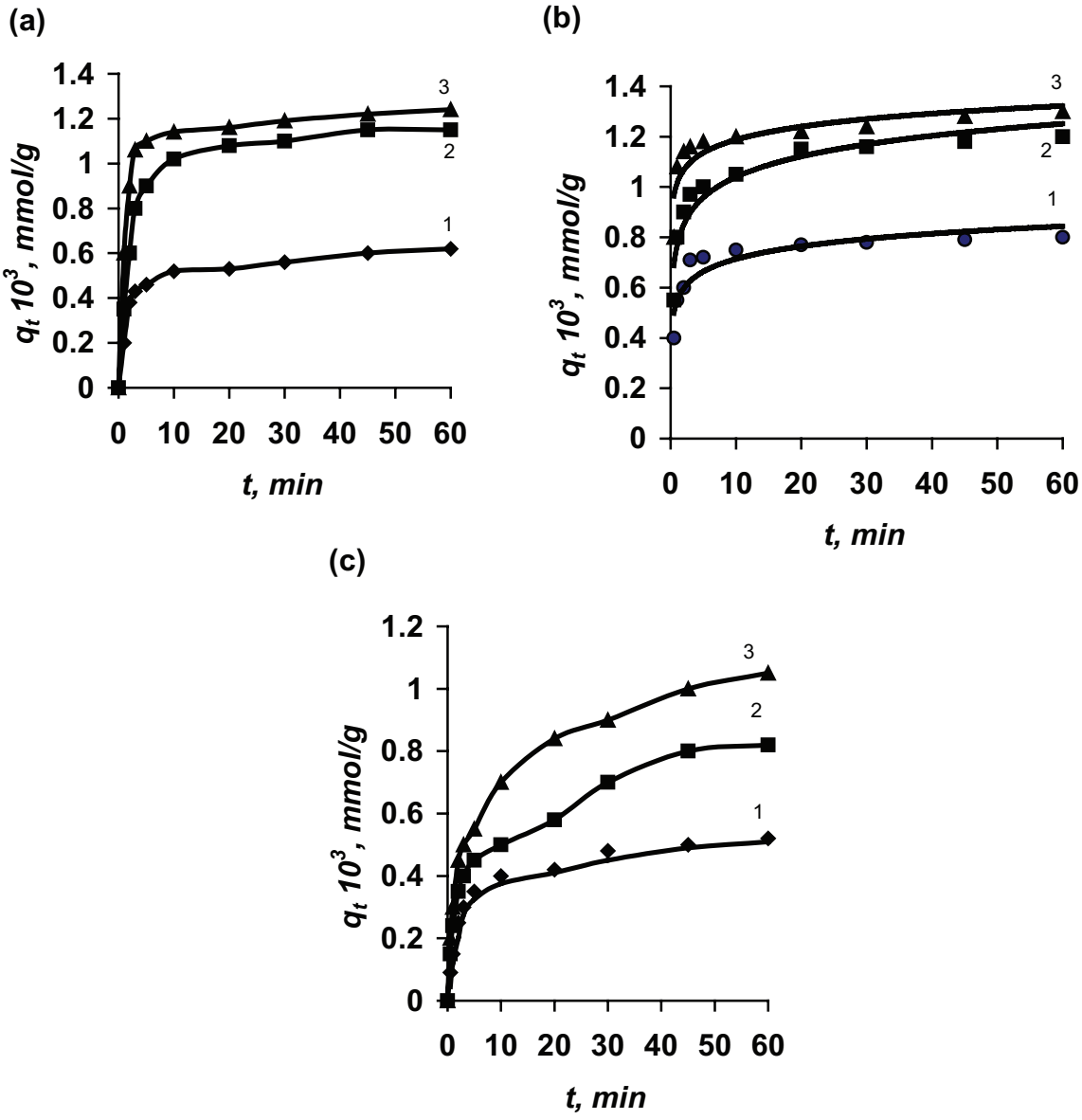

Fig. 5. Kinetic curves for the adsorption of dye LnCr on Purolite S930 at pH = 2 (a) and on Purolite A847 at pH = 2 (b) and at pH =7 (c) at different temperatures: (1) 20°C; (2) 40°C; (3) 60°C. Initial LnCr dye concentration is 0.01 mmol/L.

the fact that a large number of surface sites are available for sorption at the beginning of the process and, after a lapse of time, the remaining sites are difficult to occupy because of repulsion between LnCr molecules of the solid and bulk phases.

On the other hand, the value of q_t of LnCr depends on temperature and indicates the mobility of the dye molecule, which increases with increase in temperature. Whereas thermodynamic investigations are used to evaluate the nature of sorption (physical or chemical), the thermodynamic parameters such as the Gibbs free energy change $\Delta G°$ (kJ mol^{-1}), standard enthalpy change $\Delta H°$ (kJ mol^{-1}) and standard entropy change $\Delta S°$ (J mol^{-1} K^{-1}) were calculated. Accuracy estimation of the thermodynamic parameters is directly dependent on the equilibrium constant between two phases (K_C is dimensionless). Assuming that the activity coefficients are unity at low concentrations (in the Henry's law sense), thermodynamical parameters were calculated as follows [55,56]:

$$K_c = \frac{C_0 - C_e}{C_e} \tag{6}$$

$$\Delta G° = -RT \ln K_c \tag{7}$$

$$\ln K_c = \frac{\Delta S^0}{R} - \frac{\Delta H^0}{RT} \tag{8}$$

where K_c is the equilibrium constant, C_0 and C_e the initial and equilibrium solution concentration, mmol/L, respectively. R is the gas constant (8.314 J/mol K). $\Delta H°$ and $\Delta S°$ were obtained from the linear van't Hoff plot of $\ln K_c$ vs. $1/T$ and presented in Table 4.

The negative values of $\Delta S°$ and $\Delta G°$, as specified in publication [57], refer to the chemical sorption process, when the binding of an ion takes place at the solid surface, and the rotational and translation freedoms of the solute are reduced. For ion exchange, the Gibbs free energy change ($\Delta G°$) must be negative, which in turn requires the enthalpy change to be negative, because $\Delta G = \Delta H - T\Delta S$. The enthalpy $\Delta H°$ negative values obtained at all the investigated temperatures indicate the exothermic nature of the process. It is generally considered that adsorption processes are exothermic due to the heat released after bond formation between the solute and adsorbent. Moreover, $\Delta H°$ values are inside the range of physical adsorption (from 2.1 to –20.9 kJ mol^{-1}), which is possible due to the interaction between the chemical structures of LnCr and Purolite S930 or Purolite A847. The degree of chaos of the sorption system which is characterized by the entropy $\Delta S°$ value is lower at pH = 2 than that at pH = 7 for both the investigated sorbents Purolite S930 and Purolite A847 (Table 4). A decrease in the negative value of $\Delta G°$ with an increase in temperature indicates that the adsorption process on Purolite S 930 is more favorable at lower temperatures. An increase in the negative value of $\Delta G°$ with an increase in temperature obtained for Purolite A847 implies that lower temperatures make the adsorption easier. Therefore, the adsorption of LnCr dye by Purolite S930 and Purolite A847 can be ascribed to physical–chemical (ion exchange) adsorption processes rather than pure physical or chemical adsorption processes.

Table 4
Thermodynamic parameters for sorption of dye on Purolite S930 and Purolite A847

pH	$\Delta H°$ (kJ mol^{-1})	$\Delta S°$ (J K^{-1} mol^{-1})	$\Delta G°$ (kJ mol^{-1})		
			T = 293 K	T = 313 K	T = 333 K
Purolite S930					
2	–17.29	–45.09	–4.43	–2.36	–2.73
7	–4.31	–11.58	–1.01	–0.49	–0.57
Purolite A847					
2	–7.91	–32.18	–1.46	–2.27	–2.73
7	–4.90	–18.9	–0.60	–1.08	–1.34

Higher negative values of ΔH at solution pH 2 compared with those at pH 7 testify more spontaneous sorption in acidic media.

Thus, these data prove that LnCr dye sorption on Purolite S930, as on Purolite A847, is a thermodynamically exothermic, spontaneous reaction, which takes place through chemical (ion exchange)–physical sorption on both exchangers.

3.3. Equilibrium and kinetic studies

To optimize the design of the sorption system for the removal of LnCr from wastewater is important to establish the models, corresponding to the experimental equilibrium and kinetic curves.

Analysis of the isotherms data allows ascertaining the maximum capacity of the sorbent, estimating the surface properties and formulating an equation for effective design of the sorption system. The data of obtained isotherms, presented in Fig. 4 were fitted by the well-known isotherm models, namely the Langmuir [58,59] and Freundlich ones [60].

The Langmuir model assumed that the adsorption proceeds on monolayer (the adsorbed layer is one molecule in thickness), whereas the Freundlich model describes the adsorption on heterogeneous surfaces and is suitable not only in the case of the monolayer coverage [61–63].

The linear forms of the applicable isotherms equations are given in Table 5 whereas the calculated sorption isotherms parameters for LnCr sorption on chelating Purolite S930 and anion exchanger Purolite A847 are given in Table 5. The error, arising from the transformation of the non-linear isotherm equation to the linear form was characterized by the coefficient of correlation (R^2).

Table 6 shows that the sorption of LnCr on Purolite S930 at pH = 7 fitted with the Langmuir and Freundlich isotherm has a low value of R^2 confirming that both the isotherms cannot represent the sorption process. Conversely, the Langmuir and Freundlich isotherms well enough represent LnCr sorption on Purolite S930 at pH = 2 and on Purolite A847 at pH = 2 and pH = 7. However, the R^2 values for Langmuir isotherm higher than that for the Freundlich isotherm model suggest that the LnCr sorption proceeds on the monolayer of Purolite A847. Whereas somewhat higher R^2 values obtained for the Freundlich isotherm model for the LnCr sorption on Purolite S930 at pH = 2 allow assuming that the sorption proceeds both on the monolayer and on heterogeneous surfaces.

The dimensionless separation factor $R_L = 1/(1 + K_L C_0)$ based on the Langmuir constant falls within the 0–1 range, which confirms that the LnCr sorption is favorable both on Purolite S930 (at pH = 2) and Purolite A847 (at pH = 2 and pH = 7). Besides, the parameter $1/n$ in the Freundlich model refers to the adsorption intensity. The value of $1/n$ was in the range of 0.23 to 0.91 (Table 5) which suggests favorable LnCr sorption both for Purolite S930 and Purolite A847 according to $0 < 1/n < 1$ [61–63].

Analysis of the kinetic data allows determining the adsorbent uptake rate for effective design of the sorption system. Therefore, the experimental kinetic data obtained for the LnCr adsorption on Purolite S930 and Purolite A847 were assessed using the pseudo first- and second-order kinetic models [64–66] and intraparticle diffusion model by Weber and Morris [67–69]. The linear forms of the applicable kinetic models equation are given in Table 7, whereas the calculated first-order kinetic and second-order kinetic parameters for chelating Purolite S930 and anion exchanger Purolite A847 are given in Tables 8 and 9, respectively. The correlation coefficients (R^2) for both adsorbents have higher values for the pseudo second-order kinetic model compared with those for pseudo first-order kinetic model, which confirms better compliance of the former model with experimental data.

The calculated adsorption capacity q_{eq} (μmol g^{-1}) in the case of the pseudo second-order model was very close to the measured one, which also confirmed the high accordance of the measured data to the model. The pseudo second-order rate constant k_2 for the LnCr dye sorption on Purolite S930 with an increase in solution temperature from 20°C to 60°C

Table 5
Linear expressions of adsorption isotherms

Isotherm	Linear expression	Plot	Parameters
Langmuir	$\frac{1}{q_{eq}} = \frac{1}{q_L} + \frac{1}{q_L K_L}\left(\frac{1}{C_e}\right)$	$1/q_{eq}$ vs. $1/C_e$	Equilibrium sorption q_L = 1/intercept; Langmuir constant K_L = slope $(1/q_L.K_L)$
Freundlich	$\ln q_{eq} = \ln K_F + \frac{1}{n}\ln C_e$	$\ln q_{eq}$ vs. $\ln C_e$	Freundlich constant K_F = exp (intercept); Intensity of the sorption n = 1/slope

Table 6
Langmuir and Freundlich model parameters obtained for LnCr sorption on Purolite S930 and Purolite A847

Parameter	Purolite S930		Purolite A847	
	pH = 2	pH = 7	pH = 2	pH = 7
Langmuir model				
K_l (g μmol^{-1})	317	–6.44	4,703	296
q_L (μmol g^{-1})	0.89	–6.47	2.4	2.2
R^2	0.986	0.808	0.982	0.984
$R_L = 1/(1 + K_L C_o)$	0.86		0.30	0.87
Freundlich model				
K_F (μmol g^{-1})	0.324	0.224	0.1148	0.2042
$1/n$	0.76	0.91	0.23	0.71
R^2	0.990	0.786	0.929	0.955

Table 7
Linear expressions of adsorption kinetic models

Kinetic model	Linear expression	Plot order	Parameters
Pseudo first-order	$\ln(q_{eq,exp} - q_t) = \ln q_{eq,calc} - k_1 t$	$\ln(q_{eq} - q_t)$ vs. t	Pseudo first-order rate constant k_1 = slope $q_{eq,\,calc}$ = exp(intercept)
Pseudo second-order	$\frac{t}{q_t} = \frac{1}{k_2 q_{eq,calc}^2} + \frac{1}{q_{eq,calc}} t$	t/q_t vs. t	$q_{eq,calc}$ = 1/slope Pseudo second-order rate constant k_2 = slope^2/intercept
Intraparticle diffusion (by Weber and Morris)	$q_t = k_i\left(t^{0,5}\right) + \mathrm{B}$	q_t vs. $t^{0.5}$	Intraparticle diffusion rate constant k_i = slope Boundary layer thickness B = intercept

Table 8
Pseudo first-order- and second-order-kinetic models parameters for LnCr adsorption on Purolite S930

T (°C)	pH	$q_{eq,exp}$ (μmol g^{-1})	Pseudo first-order kinetics			Pseudo second-order kinetics		
			k_1 (min^{-1})	$q_{eq,calc}$ (μmol g^{-1})	R^2	k_2 (g μmol^{-1} h^{-1})	$q_{eq,calc}$ (μmol g^{-1})	R^2
20	2	0.97	0.002	0.55	0.906	0.805	0.62	0.998
	7	0.31	0.003	0.41	0.912	0.724	0.38	0.995
40	2	1.23	0.015	0.26	0.950	0.863	1.23	0.998
	7	0.31	0.015	0.18	0.881	0.621	0.31	0.997
60	2	1.32	0.011	0.25	0.886	1.108	1.30	0.998
	7	0.37	0.013	0.26	0.789	0.169	0.39	0.966

Table 9
Pseudo first-order- and second-order-kinetic model parameters for LnCr adsorption on Purolite A847

T (°C)	pH	$q_{eq,exp}$ (μmol g^{-1})	Pseudo first-order kinetics			Pseudo second-order kinetics		
			k_1 (min^{-1})	$q_{eq,calc}$ (μmol g^{-1})	R^2	k_2 (g μmol^{-1} h^{-1})	$q_{eq,calc}$ (μmol g^{-1})	R^2
20	2	0.82	0.060	0.023	0.905	1.67	0.8	0.999
	7	0.50	0.035	0.025	0.810	0.423	0.5	0.997
40	2	1.19	0.017	0.024	0.918	1.466	1.2	0.999
	7	0.89	0.0213	0.0439	0.967	0.096	1.0	0.971
60	2	1.32	0.0138	0.0238	0.747	1.231	1.3	0.999
	7	1.05	0.0257	0.0448	0.985	0.162	1.1	0.997

indicates an increase from 0.805 to 1.108 g/ (μmol min) at pH ≤ 2 and decrease from 0.724 to 0.169 g/(μmol min) at pH ≥ 7, whereas the equilibrium adsorption capacity q_{eq} increases with increasing temperature (Table 8).

However k_2 values for the LnCr dye adsorption onto Purolite A847 with an increase in temperature decrease from 1.67 to 1.213 g/(μmol min) at pH ≤ 2 and from 0.423 to 0.162 g/(μmol min) at pH 7, whereas the equilibrium adsorption capacity increases (Table 8).

Consequently, it may be concluded that the LnCr adsorption mechanism onto both adsorbents does not exclusively follow the physical sorption mechanism when generally an increase in temperature increases the rate of attainment of equilibrium and decreases the equilibrium adsorption, but other processes including chemical adsorption also occur [17,18,70].

From the kinetic parameters k_2 at different temperatures, the activation energies, representing the minimum energy that the dye-anion exchanger system should have for the reaction of adsorption to proceed, were estimated using the Arrhenius relationship [70]:

$$\ln k_2 = \ln A - \frac{E_a}{RT} \tag{9}$$

where E_a is the Arrhenius activation energy of adsorption, A is the Arrhenius factor, R is the gas constant equal to 8.314 J/mol K, and T is the solution temperature. When $\ln k_2$ is plotted against $1/T$, a straight line with a slope of $-E_a/R$ was obtained. The negative and negligible values of E_a obtained for chelating Purolite S930 at pH = 2 (–11.22 J mol^{-1}) and at pH = 7 (–37.91 J mol^{-1}) indicated the exothermic nature of the adsorption process and the physical adsorption with relatively weak attraction forces. Whereas the negative values of E_a calculated for Purolite A847 at pH = 2 (–6.16 kJ mol^{-1}) and at pH=7 (–20.33 kJ/mol) favor again the simultaneous physical–chemical exothermic adsorption.

To analyze the rate controlling step such as the mass transport or chemical reaction processes is very beneficial to specify the sorption mechanism. It is universally accepted that adsorption takes place by a multistep mechanism of which most important are diffusion across the liquid film surrounding the sorbent particles (the process controlled by an external mass transfer) and the diffusion within the particle itself assuming the pore diffusion mechanism (the process controlled by intraparticle diffusion) and then physical or chemical adsorption at the site [71].

The intraparticle diffusion model equation by Weber and Morris (Table 7) was selected for evaluation of the diffusion processes mentioned above. According to this model the plot of q_t vs. the square root of time ($t^{0.5}$) would be linear, if intraparticle diffusion were involved in the adsorption process, and if these lines passed through the origin, intraparticle diffusion would be the rate determining step [68,69]. However, the plots obtained for both the Purolite S930 and Purolite A847 sorbents show two different linearity profiles with different slopes (k_{i-1} and k_{i-2}) (Fig. 6) suggesting that the intraparticle diffusion is not the rate limiting step for the whole reaction. The rate constants for the intraparticle diffusion values k_{i-1} and k_{i-2} are presented in (Table 10).

The first steep linear portion of plots q_t against $t^{0.5}$ can be attributed to the diffusion of LnCr through the solution to the external surface of the resin, or the boundary layer diffusion of the dye molecules (the intraparticle diffusion rate constant k_{i-1}). The second section is the gradual sorption stage, where intraparticle diffusion is rate-controlled (the intraparticle

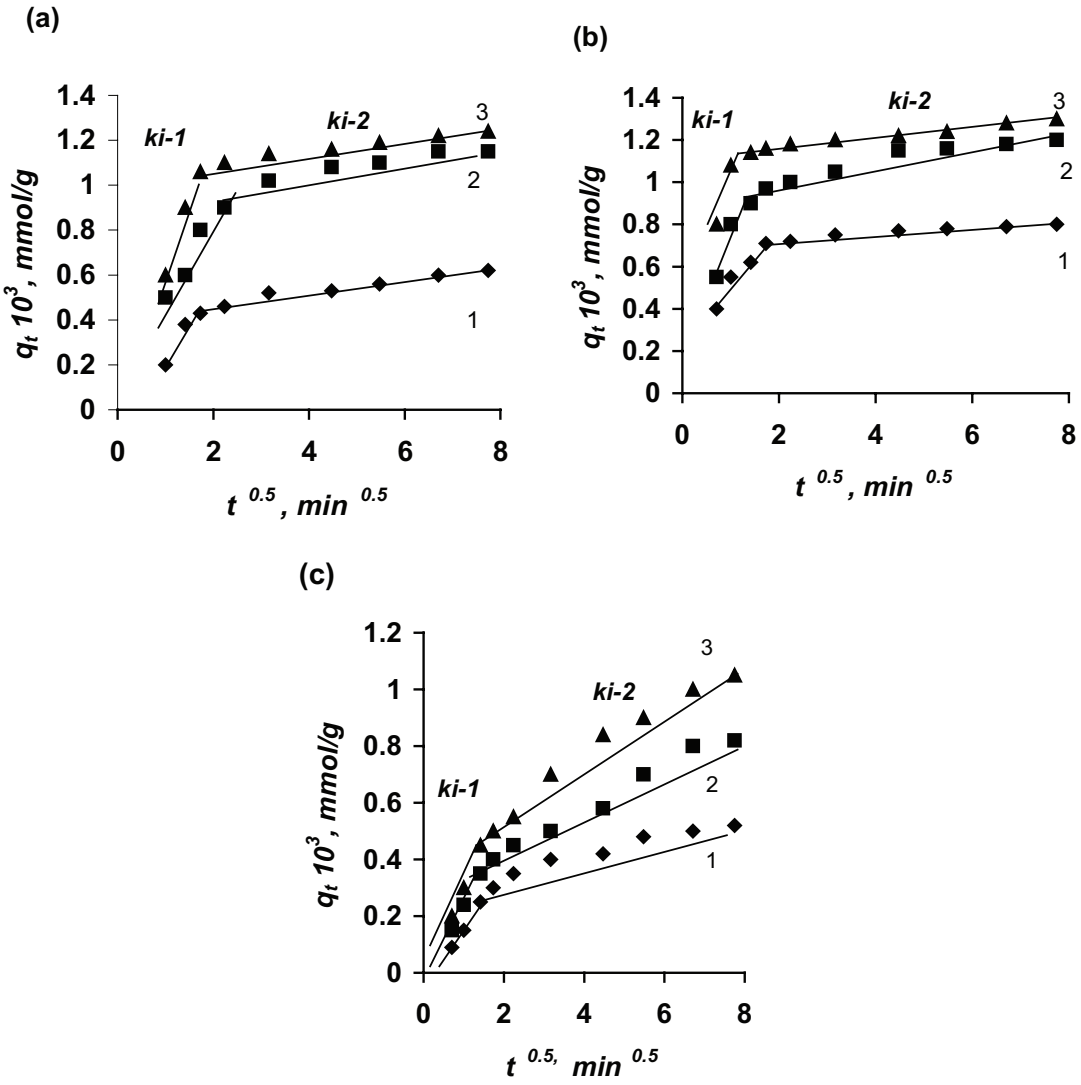

Fig. 6. Intraparticle diffusion model for LnCr dye sorption at solution pH = 2 on Purolite S 930 (a) and Purolite A847 (b); (c) on Purolite A847 at solution pH = 7. The temperature of the solution: (1) 20°C; (2) 40°C; (3) 60°C.

Table 10
Intraparticle diffusion parameters k_{i-1}, k_{i-2} (μmol g^{-1} min$^{-0.5}$) and B_1, B_2 (μmol g^{-1})

Temperature (°C)	pH	k_{i-1}	B_1	R_1^2	k_{i-2}	B_2	R_2^2
Purolite S930							
20	2	0.256	0.012	0.974	0.027	0.413	0.959
40		0.449	0.009	0.988	0.042	0.857	0.965
60		0.619	0.002	0.998	0.024	1.052	0.986
Purolite A847							
20	2	0.455	0.037	0.956	0.014	0.6934	0.940
	7	0.173	0.101	0.970	0.2477	0.008	0.993
40	2	0.663	0.044	0.961	0.0392	0.925	0.914
	7	0.247	0.008	0.993	0.0737	0.275	0.983
60	2	0.846	0.094	0.924	0.0225	1.124	0.989
	7	0.316	0.009	0.995	0.093	0.321	0.971

diffusion rate constant k_{i-2}) [72]. The larger slopes of the first sharp linear portion (k_{i-1}) indicate that the rate of LnCr dye adsorption is higher at the initial stage due to the instantaneous availability of large surface area and active adsorption sites. The lower slopes of the second linear portion (k_{i-2}) are due to decreased concentration gradients that make dye diffusion in the micropores of the resin take a long time, thus leading to a low removal rate.

The values of intercept B indirectly represent the boundary layer effect [56]. The larger B value represents a greater effect of the boundary layer on the diffusion. Thus, the larger value of the intercept B_2 than B_1 at all temperatures obtained for Purolite S930 and Purolite A847 shows a more pronounced effect on the intraparticle diffusion stage that controls the adsorption rate (Table 10). The larger slopes of Purolite A847 are higher at the beginning due to instantaneous availability of a larger surface and active adsorption sites. It should be noted that k_{i-2} depended more on the concentration of active sites in the sorbent rather than on the sorbent structure (Fig. 7).

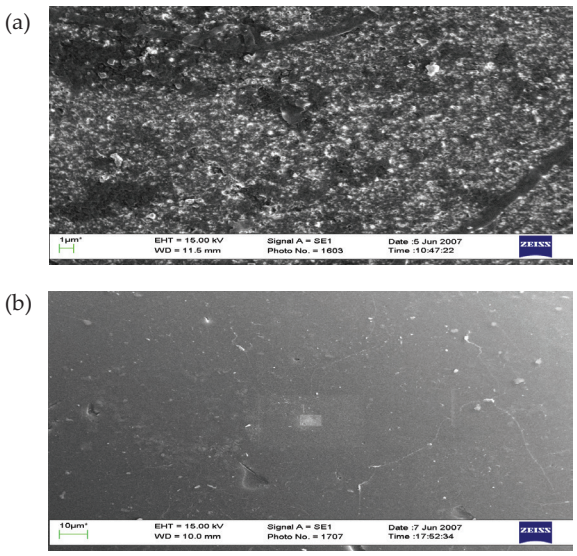

Fig. 7. Scanning electron micrographs of the bead cross-section of Purolite S 930 (a) and Purolite A847 (b) at 10,000× magnification.

Although, the macroporous Purolite S 930 is characterized by a larger BET surface area (20.6 m^2/g) when compared with that of the gel structure Purolite A847 (4.05 m^2/g), the equilibrium sorption capacity q_L was lower (0.89 and 2.4 μmol/g, respectively).

Moreover, the intraparticle diffusion rate constants depended on temperature increase, which suggests that the external mass transfer and intraparticle diffusion are co-acting during the LnCr dye sorption onto the chelating Purolite S 930 resin. It is worthy of note that the compositions of wastewaters can vary widely due to the variety of technologies and materials [73]. Wastewaters from dyeing processes are intensively colored and have many chemicals such as sodium chloride, sodium sulfate, sodium hydroxide, detergents and other inorganic and organic auxiliaries [74]. As mentioned above, different anion exchangers (strong and weakly basic with gel or macroporous structures of styrene-divinylbenzene or acrylic matrices) are employed for the removal of acid and reactive dye anions [10–19]. Yet, when a metal complex dye is used, free heavy metal ions (Cr, Cu, Al, Sb, Ti) from the raw materials used in dye manufacture) can possibly ingress into wastewater. According to the present study, the chelating Purolite S930 resin is effective in the removal of the LnCr dye anions. Consequently, chelating resins, including Purolite S930, due to their unique properties depending on solution pH such as anionic, cationic or amphoteric seem to be effective in the simultaneous removal of dye anions and heavy metal cations. Therefore, the simultaneous removal of anionic dye and heavy metal ions by commercial chelating ion exchange resins needs to be investigated.

4. Conclusions

The abilities of the macroporous chelating resin containing iminodiacetic groups (Purolite S930) and the weak basic anion exchanger Purolite A847 to remove the chromium complex dye (LnCr) from aqueous solutions in the batch system have been compared. It has been determined that the characteristic properties of Purolite S930 are less favorable for the removal of LnCr than those of Purolite A847.

The extent of removal of LnCr using Purolite S930 depended on solution pH and was about 1.8 – 2.5 times greater at pH = 2 as compared with that at pH = 7.

The Langmuir and Freundlich isotherms represent adequately LnCr sorption on Purolite S930 at pH = 2 and on Purolite A847 at pH = 2 and pH = 7 suggesting that the sorption proceeds not only on monolayer coverage but also on heterogeneous surfaces. The maximum adsorption capacities calculated from the Langmuir isotherm, the best fit model to the experimental data, for Purolite S930 and Purolite A847 at pH = 2 are 0.89 and 2.4 μmol g^{-1}, respectively.

The pseudo second-order kinetic model is well suited to the description of the experimental kinetic data. The dye removal using both chelating Purolite S 930 and anion exchanger Purolite A847, according to the kinetic (E_a, k_2, k_i) and thermodynamic ($\Delta G°$, $\Delta H°$, $\Delta S°$) parameters and FTIR spectra, is the simultaneous physical and chemical (ion exchange) sorption at co-acting external mass transfer and intraparticle diffusion.

Acknowledgments

The authors thank the Purolite International Ltd. (UK) for providing the anion exchanger Purolite A847 and chelating resin Purolite S930, the Clariant (Switzerland) for the Lanasyn Navy M-DNL dye. The authors gratefully acknowledge the assistance of Dr. Irena Mirvienė in language editing and proofreading.

References

[1] K. Hunger, Ed., Industrial Dyes. Chemistry, Properties, Application, Wiley-VCH, Weinheim, 2003.
[2] Brochure Clariant Product, 2014. https://www.clariant.com/en/Business-Units/Pigments/Special.../Aluminium-Finishing.
[3] T. Poiger, S.D. Richardson, G.L. Baughman, Analysis of anionic metallized azo and formazan dyes by capillary electrophoresis-mass spectrometry, J. Chromatogr. A, 886 (2000) 259–270.
[4] V.M. Correia, T. Stephenson, S.J. Judd, Characterization of textile wastewater – a review, Environ. Technol., 15 (1994) 917–926.
[5] S.F. Dubow, G.D. Boardmen, D.J. Michelsen, in A. Reife, H.S. Freemqan, Environmental Chemistry of Dyes and Pigments, Wiley, USA, 1996.
[6] Environmental Agency, Guidance for Textile sector, Integrated Pollution Prevention and Control (IPPC), IPPC S6.05, 2002.
[7] C. Allegre, P. Moulin, M. Maisseu, G.L. Charbit, Treatment and reuse of reactive dyeing effluents, J. Membr. Sci., 269 (2006) 15–34.
[8] V. Dulman, C. Simion, A. Bârsănescu, I. Bunia, V. Neagu, Adsorption of anionic textile dye Acid Green 9 from aqueous solution onto weak or strong base anion exchangers, J. Appl. Polym, Sci., 113 (2009) 615–627.
[9] A. Masoumi, M. Ghaemy, Adsorption of heavy metal ions and azo dyes by crosslinked nanochelating resins based on poly(methylmethacrylate-co-maleic anhydride, Express Polym. Lett., 8 (2014) 187–196.
[10] M. Wawrzkiewicz, Z. Hubicki, Removal of tartrazine from aqueous solutions by strongly basic polystyrene anion exchange resins, J. Hazard. Mater., 164 (2009) 502–509.
[11] M. Leszczynska, Z. Hubicki, Application of weakly and strongly basic anion exchangers for the removal of Brilliant Yellow from aqueous solutions, Desal. Wat. Treat., 2 (2009) 156–161.
[12] M. Wawrzkiewicz, Z. Hubicki, Kinetic studies of dyes sorption from aqueous solutions onto the strongly basic anion-exchanger Lewatit MonoPlus M-600, Chem. Eng. J., 150 (2009) 509–515.

[13] M. Wawrzkiewicz, Z. Hubicki, Equilibrium and kinetic studies on the adsorption of acidic dye by the gel anion exchanger, J. Hazard. Mater., 172 (2009) 868–874.
[14] M. Greluk, Z. Hubicki, Sorption of SPADNS azo dye on polystyrene anion exchangers: equilibrium and kinetic studies, J. Hazard. Mater., 172 (2009) 280–297.
[15] S. Dragan, M. Cristea, A. Airinei, I. Poinescu, C. Luca, Sorption of aromatic compounds on macroporous anion exchangers based on polyacrylamide: relation between structure and sorption behavior, J. Appl. Polym. Sci., 55 (1995) 421–430.
[16] M. Wawrzkiewicz, Sorption of Sunset Yellow dye by weak base anion exchanger – kinetic and equilibrium studies, Environ. Technol., 32 (2011) 445–465.
[17] D. Kaušpėdienė, E. Kazlauskienė, A. Selskienė, Removal of chromium complex dye from aqueous solution using strongly basic and weakly basic anion exchangers, Ion Exchange Lett., 3 (2010) 19–24.
[18] D. Kaušpėdienė, A. Gefenienė, E. Kazlauskienė, R. Ragauskas, A. Selskienė, Simultaneous removal of azo and phthalocyanine dyes from aqueous solutions using weak base anion exchange resin, Water Air Soil Pollut., 224 (2013) 1769–1781.
[19] D.B. Prelot, A. Geneste, L. Ch. De Menorval, J. Zajac, Removal of three anionic orange-type dyes and Cr(VI) oxyanion from aqueous solutions onto strongly basic anion-exchange resin, The effect of single-component and competitive adsorption, Colloids Surf. A, 508 (2016) 240–250.
[20] H. Javadian, M. Torabi Angaji, M. Naushad, Synthesis and characterization of polyaniline/γ-alumina nanocomposite: a comparative study for the adsorption of three different anionic dyes, J. Ind. Eng. Chem., 20 (2014) 3890–3900.
[21] D. Pathania, G. Sharma, A. Kumar, Mu. Naushad, S. Kalia, A. Sharma, Z.A. Alothman, Combined sorptional photocatalytic remediation of dyes by polyaniline Zr(IV) selenotungstophosphate nanocomposite, Toxicol. Environ. Chem., 97 (2015) 526–537.
[22] A.A. Alqadami, M. Naushad, M.A. Abdalla, M.R. Khan, Z.A. Alothman, Adsorptive removal of toxic dye using Fe_3O_4–TSC nanocomposite: equilibrium, kinetic, and thermodynamic studies, J. Chem. Eng. Data, 61 (2016) 3806–3813.
[23] T.A. Arica, E. Ayas, M.Y. Arica, Magnetic MCM-41 silica particles grafted with poly(glycidylmethacrylate) brush: modification and application for removal of direct dyes, Microporous Mesoporous Mater., 243 (2017) 164–175.
[24] E. Daneshvar, A. Vazirzadeh, A. Niazi, M. Kousha, M. Naushad, A. Bhatnagar, Desorption of Methylene blue dye from brown macroalga: effects of operating parameters, isotherm study and kinetic modeling, J. Clean. Prod., 152 (2017) 443–453.
[25] G. Bayramoglu, M.Y. Arica, Adsorption of Congo Red dye by native amine and carboxyl modified biomass of *Funalia trogii*: isotherms, kinetics and thermodynamics mechanisms, Korean J. Chem. Eng., 35 (2018) 1303–1311.
[26] A.B. Albadarin, M. Charara, B.J.A. Tarboush , M.N.M. Ahmad, T.A. Kurniawan, M. Naushad, G.M. Walker, Ch. Mangwandi, Mechanism analysis of tartrazine biosorption onto masau stones; a low cost by-product from semi-arid regions, J. Mol. Liq., 242 (2017) 478–483.
[27] A.B. Albadarin, M.N. Collins, M. Naushad, S. Shirazian, G. Walker, C. Mangwandi, Activated lignin-chitosan extruded blends for efficient adsorption of methylene blue, Chem. Eng. J., 307 (2017) 264–272.
[28] A. Sharma, G. Sharma, M. Naushad, A.A. Ghfar, D. Pathania, Remediation of anionic dye from aqueous system using bio-adsorbent prepared by microwave activation, Environ. Technol., 39 (2018) 917–930.
[29] G. Bayramoğlu, V. Cengiz Ozalp, M. Yakup Arıca, Removal of Disperse Red 60 dye from aqueous solution using free and composite fungal biomass of *Lentinus concinnus*, Water Sci. Technol., 75 (2016) 366–377.
[30] G. Bayramoglu, A. Akbulut, G. Liman, M.Y. Arica, Removal of metal complexed azo dyes from aqueous solution using tris(2-aminoethyl)amine ligand modified magnetic p(GMA-EGDMA) cationic resin: adsorption, isotherm and kinetic studies, Chem. Eng. Res. Des., 124 (2017) 85–97.
[31] S.K. Sahni, J. Reedijk, Coordination chemistry of chelating resins and ion exchangers, Coord. Chem. Rev., 59 (1984) 1–139.
[32] B. Busche, R. Wiacek, J. Davidson, V. Koonsiripaiboon, W. Yantasee, R.S. Addleman, G.E. Fryxell, Synthesis of nanoporous iminodiacetic acid sorbents for binding transition metals, Inorg. Chem. Commun., 12 (2009) 312–315.
[33] Z. Hubicki, D. Kolodynska, Selective removal of heavy metal ions from waters waste waters using ion exchange methods, in Ion Exchange Technologies, InTech, 2012, pp. 193–240.
[34] M. Marhol, K.L. Cheng, Some chelating ion-exchange resins containing ketoimino carboxylic acids as functional groups, Talanta, 21 (1974) 751–762.
[35] S.A. Cavaco, S. Fernandes, C.M. Augusto, M.J. Quina, L.M. Gando-Ferreira, Evaluation of chelating ion-exchange resins for separating Cr(III) from industrial effluents, J. Hazard. Mater., 169 (2009) 516–523.
[36] F. Gode, E. Pehlivan, A comparative study of two chelating ion-exchange resins for the removal of chromium(III) from aqueous solution, J. Hazard. Mater., 100 (2003) 231–243.
[37] W. Wei, B. Zhao, M. He, B. Chen, B. Hu, Iminodiacetic acid functionalized magnetic nanoparticles for speciation of Cr(III) and Cr(VI) followed by graphite furnace atomic absorption spectrometry detection, RSC Adv., 7 (2017) 8504–8511.
[38] S. Hirataa, U.K. Hondab, O. Shikinob, N. Maekawac, M. Aiharac, Determination of chromium_III and total chromium in seawater by on-line column preconcentration inductively coupled plasma mass spectrometry, Spectrochim. Acta, Part B, 55 (2000) 1089–1099.
[39] Z. Zainol, M. Nicol, Ion-exchange equilibria of Ni^{2+}, Co^{2+}, Mn^{2+} and Mg^{2+} with iminodiacetic acid chelating resin Amberlite IRC 748, Hydrometallurgy, 99 (2009) 175–180.
[40] A. Yuchi, T. Sato, Y. Morimoto, H. Mizuno, H. Wada, Adsorption mechanism of trivalent metal ions on chelating resins containing iminodiacetic acid groups with reference to selectivity, Anal. Chem., 69 (1997) 2941–2944.
[41] H. Hashemi-Moghaddam, Z. Noshiri, Removal of cyanide and zinc–cyanide complex with malachite green functionalized amberlite XAD-4 resin from electroplating wastewater, Desal. Wat. Treat., 53 (2015) 2481–2488.
[42] P.R. Gogate, A.B. Pandit, A review of imperative technologies for wastewater treatment I: oxidation technologies at ambient conditions, Adv. Environ. Res., 8 (2004) 501–551.
[43] J.T. Kanzelmeyer, C.D. Adams, Removal of Copper from a Metal-Complex Dye by Oxidative Pretreatment and Ion Exchange, Water Environ. Res., 68 (1996) 222–228.
[44] V. Baublytė, L. Čečiotkiene, B. Baltrušaite, A. Gefeniene, E. Kazlauskiene, D. Kaušpėdiene, A. Selskiene, Removal of copper phthalocyanine dye from aqueous solutions, Chem. Technol., 2 (2010) 54–61.
[45] Ch. Y. Kim, H.M. Choi, H.T. Cho, Effect of deacetylation on sorption of dyes and chromium on chitin, J. Appl. Polym. Sci., 63 (1998) 725–736.
[46] G.K. Zoorob, J.A. Caruso, Speciation of chromium dyes by high-performance liquid chromatography with inductively coupled plasma mass spectrometric detection, J. Chromatograph. A, 773 (1997) 157–162.
[47] Technical data for Purolite S930, Purolite International Co., Ltd. Available at: https://puroweb.purolite.com.
[48] Technical data for Purolite A847, Purolite International Co., Ltd. Available at: https://puroweb.purolite.com.
[49] N. Sakkayawong, P. Thiravetyan, W. Nakbanpote, Adsorption mechanism of synthetic reactive dye wastewater by chitosan, J. Colloid Interface Sci., 286 (2005) 36–42.
[50] A.A. Zagorodni, D.L. Kotova, V.F. Selemenev, Infrared spectroscopy of ion exchange resins: chemical deterioration of the resins, React. Funct. Polym., 53 (2002) 157–171.
[51] Z.W. Ming, C.P. Long, P.B. Cai, Z.Q. Xing, X.B. Zhang, Synergistic adsorption of phenol from aqueous solutions onto polymeric adsorbents, J. Hazard. Mater., 152 (2006) 123–129.
[52] E. Marais, T. Nyokong, Adsorption of 4-nitrophenol onto Amberlite IRA-900 modified with metallophtalocyanines, J. Hazard. Mater., 152 (2008) 293–301.

[53] X. Li, E. Puhakka, J. Ikonen, M. Söderlund, A. Lindberg, S. Holgersson, A. Martin, M. Siitari-Kauppi, Sorption of Se species on mineral surfaces, part I: batch sorption and multi-site modelling, Appl. Geochem., 95 (2018) 147–157.
[54] M. Greluk, Z. Hubicki, Effect of basicity of anion exchangers and number and positions of sulfonic groups of acid dyes on dyes adsorption on macroporous anion exchangers with styrenic polymer matrix, Chem. Eng. J., 215–216 (2013) 731–739.
[55] H.N. Tran, Sh.-J. You, H.-P. Chao, Thermodynamic parameters of cadmium adsorption onto orange peel calculated from various methods: a comparison study, J. Environ. Chem. Eng., 4 (2016) 2671–2682.
[56] C. Namasivayam, S. Senthilkumar, Adsorption of Copper(II) by "Waste" Fe(III)/Cr(III) Hydroxide from Aqueous Solution and Radiator Manufacturing Industry Wastewater, Sep. Sci. Technol., 34 (1999) 201–217.
[57] P. Saha, Sh. Chowdhury, Insight into Adsorption Thermodynamics, in: M. Tadashi, Thermodynamics, InTech, 2011, pp. 349–364.
[58] I.J. Langmuir, The adsorption of gases on plane surfaces of glass, mica and platinum, J. Am. Chem. Soc., 4 (1918) 1361–1403.
[59] R. Masel, Principles of Adsorption and Reaction on Solid Surfaces, Wiley Interscience, 1996.
[60] H.M.F. Freundlich, Über die adsorption in lösungen, Z. Phys. Chem., 57 (1906) 385–470.
[61] D. Chatzopoulos, A. Varma, R. Irvine, Activated carbon adsorption and desorption of toluene in the aqueous phase, AIChE J., 39 (1993) 2027–2041.
[62] A. Behnamfard, M.M. Salarirad, Equilibrium and kinetic studies on free cyanide adsorption from aqueous solution by activated carbon, J. Hazard. Mater., 170 (2009) 127–133.
[63] P.S. Kumar, S. Ramalingam, C. Senthamarai, M. Niranjanaa, P. Vijayalakshmi, Adsorption of dye from aqueous solution by cashew nut shell: studies on equilibrium isotherm, kinetics and thermodynamics of interactions, Desalination, 261 (2010) 52–60.
[64] S. Lagergren, Zur theorie der sogenanten adsorption gelöster stoffe, K. Sven. Vetensk.akad. Handl., 24 (1898) 1–39.
[65] Y.S. Ho, Review of second-order models for adsorption systems, J. Hazard. Mater., B136 (2006) 681–689.
[66] Sh. Wang, H. Li, Kinetic modelling and mechanism of dye adsorption on unburned carbon, Dyes Pigm., 72 (2007) 308–314.
[67] W.J. Weber, J.C. Morris, Kinetics of adsorption on carbon materials, J. Sanitary Eng. Div. Am. Soc. Civ. Eng., 89 (1963) 31–56.
[68] S.J. Allen, G. McKay, K.Y.H. Khader, Intraparticle diffusion of a basic dye during adsorption onto sphagnum peat, Environ. Pollut., 56 (1989) 39–50.
[69] F. Guzel, H. Yakut, G. Topal, Determination of kinetic and equilibrium parameters of the batch adsorption of Mn(II), Co(II), Ni(II) and Cu(II) from aqueous solution by black carrot (*Daucus carota* L.) residues, J. Hazard. Mater., 153 (2008) 1275–1287.
[70] V.J. Inglezakis, A.A. Zorpas, Heat of adsorption, adsorption energy and activation energy in adsorption and ion exchange systems, Desal. Wat. Treat., 36 (2012) 149–157.
[71] M. Sarkar, P.K. Acharya, B.J. Bhattacharya, Modeling the adsorption kinetics of some priority organic pollutants in water from diffusion and activation energy parameters, J. Colloid Interface Sci., 266 (2003) 23–32.
[72] W.H. Cheung, Y.S. Szeto, G. McKay, Intraparticle diffusion processes during acid dye adsorption onto chitosan, Bioresour. Technol., 98 (2007) 2897–2904.
[73] V.M. Correia, T. Stephenson, S.J. Judd, Characterisation of textile wastewaters – a review, Environ. Technol., 15 (1994) 917–926.
[74] M. Wawrzkiewicz, Removal of C. I. Blue 3 dye by sorption onto cation exchange resin, functionalized and non-functionalized polymeric sorbents from aqueous solutions and wastewater, Chem. Eng. J., 217 (2013) 414–425.